**Nagra**
Nationale
Genossenschaft
für die Lagerung
radioaktiver Abfälle

**Cédra**
Société coopérative
nationale
pour l'entreposage
de déchets radioactifs

**Cisra**
Società cooperativa
nazionale
per l'immagazzinamento
di scorie radioattive

# TECHNICAL REPORT 87-29

## Reflection and Tubewave Analysis of the Seismic Data from the Stripa Crosshole Site

Calin Cosma
Vibrometric OY, Finland

Suzanna Bähler
Monica Hammarström
Jörgen Pihl
National Defence Research Institute, Sweden

December 1986

Parkstrasse 23 5401 Baden/Schweiz Telephon 056/20 55 11

**Nagra**
Nationale
Genossenschaft
für die Lagerung
radioaktiver Abfälle

**Cédra**
Société coopérative
nationale
pour l'entreposage
de déchets radioactifs

**Cisra**
Società cooperativa
nazionale
per l'immagazzinamento
di scorie radioattive

# TECHNICAL REPORT 87-29

## Reflection and Tubewave Analysis of the Seismic Data from the Stripa Crosshole Site

Calin Cosma
Vibrometric OY, Finland

Suzanna Bähler
Monica Hammarström
Jörgen Pihl
National Defence Research Institute, Sweden

December 1986

Parkstrasse 23 5401 Baden/Schweiz Telephon 056/20 55 11

Der vorliegende Bericht betrifft eine Studie, die für das Stripa-Projekt ausgeführt wurde. Die Autoren haben ihre eigenen Ansichteń und Schlussfolgerungen dargestellt.Diese müssen nicht unbedingt mit denjenigen des Auftraggebers übereinstimmen.

Le présent rapport a été préparé pour le projet de Stripa. Les opinions et conclusions présentées sont celles des auteurs et ne correspondent pas nécessairement à ceux du client.

This report concerns a study which was conducted for the Stripa Project. The conclusions and viewpoints presented in the report are those of the authors and do not necessarily coincide with those of the client.

Das Stripa-Projekt ist ein Projekt der Nuklearagentur der OECD. Unter internationaler Beteiligung werden von 1980-86 Forschungsarbeiten in einem unterirdischen Felslabor in Schweden durchgeführt. Diese sollen die Kenntnisse auf folgenden Gebieten erweitern:
- hydrogeologische und geochemische Messungen in Bohrlöchern
- Ausbreitung des Grundwassers und Transport von Radionukliden durch Klüfte im Gestein
- Verhalten von Materialien, welche zur Verfüllung und Versiegelung von Endlagern eingesetzt werden sollen
- Methoden zur zerstörungsfreien Ortung von Störzonen im Fels

Seitens der Schweiz beteiligt sich die Nagra an diesen Untersuchungen. Die technischen Berichte aus dem Stripa-Projekt erscheinen gleichzeitig in der NTB-Serie der Nagra.

The Stripa Project is organised as an autonomous project of the Nuclear Energy Agency of the OECD. In the period from 1980-86, an international cooperative programme of investigations is being carried out in an underground rock laboratory in Sweden. The aim of the work is to improve our knowledge in the following areas:
- hydrogeological and geochemical measurement methods in boreholes
- flow of groundwater and transport of radionuclides in fissured rock
- behaviour of backfilling and sealing materials in a real geological environment
- non-destructive methods for location of disturbed zones in the rock

Switzerland is represented in the Stripa Project by Nagra and the Stripa Project technical reports appear in the Nagra NTB series.

Le projet Stripa est un projet autonome de l'Agence de l'OCDE pour l'Energie Nucléaire. Il s'agit d'un programme de recherche avec participation internationale, qui sera réalisé entre 1980 et 1986 dans un laboratoire souterrain, en Suède. Le but de ces travaux est d'améliorer et d'étendre les connaissances dans les domaines suivants:
- mesures hydrogéologiques et géochimiques dans les puits de forage
- chimie des eaux souterraines à grande profondeur
- écoulement des eaux souterraines et transport des radionucléides dans les roches fracturées
- comportement des matériaux de colmatage et de scellement des dépôt finals
- méthodes de localisation non destructive des zones de perturbation de la roche

La Suisse est représentée dans le projet Stripa par la Cédra. Les rapports techniques du projet Stripa sont publiés dans la série des rapports techniques de la Cédra (NTB).

## ABSTRACT

Reflection and tubewave analysis has been made using existing seismic crosshole data. The purpose of the work was to test if crosshole data are suitable for analysis by reflection and tubewave analysis methods.

The data from the crosshole research program (radar, seismics and hydraulics) in the Stripa Phase II Project resulted in the construction of a model. The results from the present study were compared to this model.

It was found that the existing data set used for tomographic analysis could only be used to a limited extent, as reflection analysis requires a more dense detector coverage. Nevertheless two reflectors were detected. The positions of the reflectors were compared to the existing crosshole model and proved to correlate well.

For the tubewave analysis almost all crosshole seismic data could be used. By comparing the results with previous hydraulic tests, it was found that tubewave sources and hydraulically conductive zones are in concordance. All previously defined zones but one could be detected.

RESUME

On a procédé à l'analyse de sismique réflexion et à celles des ondes tubulaires (tubewaves) au moyen des données existantes de sismique entre puits. Ce travail avait pour objectif de tester si les données entre puits se prêtent a ce type d'analyse.

Les données acquises avec le programme de recherche entre puits (radar, sismique et hydraulique), au cours de la phase II du projet de Stripa, ont permis d'élaborer un modèle. On a comparé les résultats de la présente étude à ce modèle.

Il s'est avéré que l'ensemble des données disponibles utilisées pour l'analyse tomographique ne pouvaient être appliquées que de manière limitée, car l'analyse de sismique réflexion nécessite une couverture plus dense de détecteurs. Deux réflecteurs ont toutefois été détectés. On a comparé leur position déterminée à l'aide du modèle entre puits et constaté qu'ils correspondent bien les uns aux autres.

Presque toutes les données sismiques entre puits ont pu être utilisées pour l'analyse des ondes tubulaires (tubewaves). En comparant les résultats aux tests hydrauliques précédents, on a constaté que les sources d'ondes tubulaires et les zones de conductivité hydraulique concordent. Toutes les zones définies précédemment ont pu être détectées, à l'exception d'une seule.

## ZUSAMMENFASSUNG

Die Daten der seismischen Durchstrahlung (Crosshole) wurden hinsichtlich reflexionsseismischer Einsätze und der B-Spülungswelleneinsätze ausgewertet, um zu testen, ob diese Daten den Anforderungen für solche Auswertungen genügen.

Die Resultate des Crosshole-Projektes aus Phase II von Stripa (Radar, Seismik, Hydraulik) wurden für den Aufbau eines Modells verwendet. Die Ergebnisse der jetzigen Studie wurden mit diesem Modell verglichen.

Es hat sich herausgestellt, dass der existierende Datensatz, der in der tomographischen Analyse verwendet wurde, nur zu einem beschränkten Teil benutzt werden konnte, da die Reflexionsanalyse eine wesentlich dichtere Aufnehmerüberdeckung erfordert. Trotzdem konnten zwei Reflektoren ermittelt werden, die mit dem obengenannten Crosshole-Modell gut korreliert werden konnten.

Für die Spülungswellenauswertung konnten alle seismischen Crosshole-Daten verwendet werden. Der Vergleich der Ergebnisse mit denen der vorhergehenden hydraulischen Tests ergab, dass die Einsätze der Spülungswellen und der hydraulisch aktiven Zonen übereinstimmten. Mit Ausnahme einer einzelnen Zone konnten alle anderen deutlich erkannt werden.

TABLE OF CONTENTS

SUMMARY

Seismic crosshole tests were performed in the Stripa mine during 1984-1986. The purpose of these tests was to detect and to characterize fracture zones by tomographic inversion (4).

The objective of the present work was to use existing tomographic data for reflection and tubewave analysis, and to compare the results with an existing model.

The experimental set-up for tomographic crosshole measurements proved not to be suitable for the reflection and tubewave analysis. The spacing between the detector distances was too long in most cases to allow a proper definition of reflectors. Each tubewave source could only be followed on a very limited number of recordings (usually not more than 7 traces).

The data used for reflection analysis refer to a part of the section between boreholes F4 and F6, where the detector spacing was 2.5 m. Signals containing most of the reflection information were sorted out for further processing, such as amplitude compensation, frequency filtering, deconvolution, move-out correction, and coherency stacking.

In the analysis, a reflector was found at the positions of zone "C", crossing the borehole F6 at 95 m and at 110 m. A weaker reflector at zone "A" was also found.

The tubewave analysis was performed on almost all tomographic data from the sections between boreholes F1-F6. The data were sorted in such a way as to get as many recorded signals as possible for each source point. The signals were bandpass filtered in order to enhance the frequencies corresponding to tubewave phases. Tubewave amplitudes were measured and compared with previous hydraulic tests. Tubewave source depths were calculated and compared to hydraulically conductive zones. All the previously defined zones, except zone "A", were detected by this kind of analysis.

The results from the reflection analysis prove that it is possible to detect reflections from fractured zones in crystalline rock and compute the position of the reflector from crosshole data.

It is also evident from the study that tubewave analysis gives an appreciation of hydraulically conductive zones.

# 1 INTRODUCTION

In the Stripa Phase II Project, seismic crosshole measurements have been performed at several occasions during the time August 1982 to February 1986. The purpose was to develop methods for rock-quality determination by tomographic analysis. Figure 1-1 shows the location of the boreholes used for the measurements (F1-F6).

In the recorded seismograms, signals which could be interpreted as reflections or tubewaves were found. The original crosshole programme in the Stripa Phase II Project could not be extended to include analysis of these later arrivals. However, at the end of that project it was decided to carry out a separate short study on the feasibilty of using later arrivals for reflection and tubewave analysis. The study was to be made on already existing data.

The present report is the result from that study, which was carried out jointly by FOA and Vibrometric OY.

The objectives of the study were:

- to enhance the visibilty of later arrivals by signal processing and display techniques
- to determine the reflector positions corresponding to the observed reflectors
- to find the sources of the tubewaves.

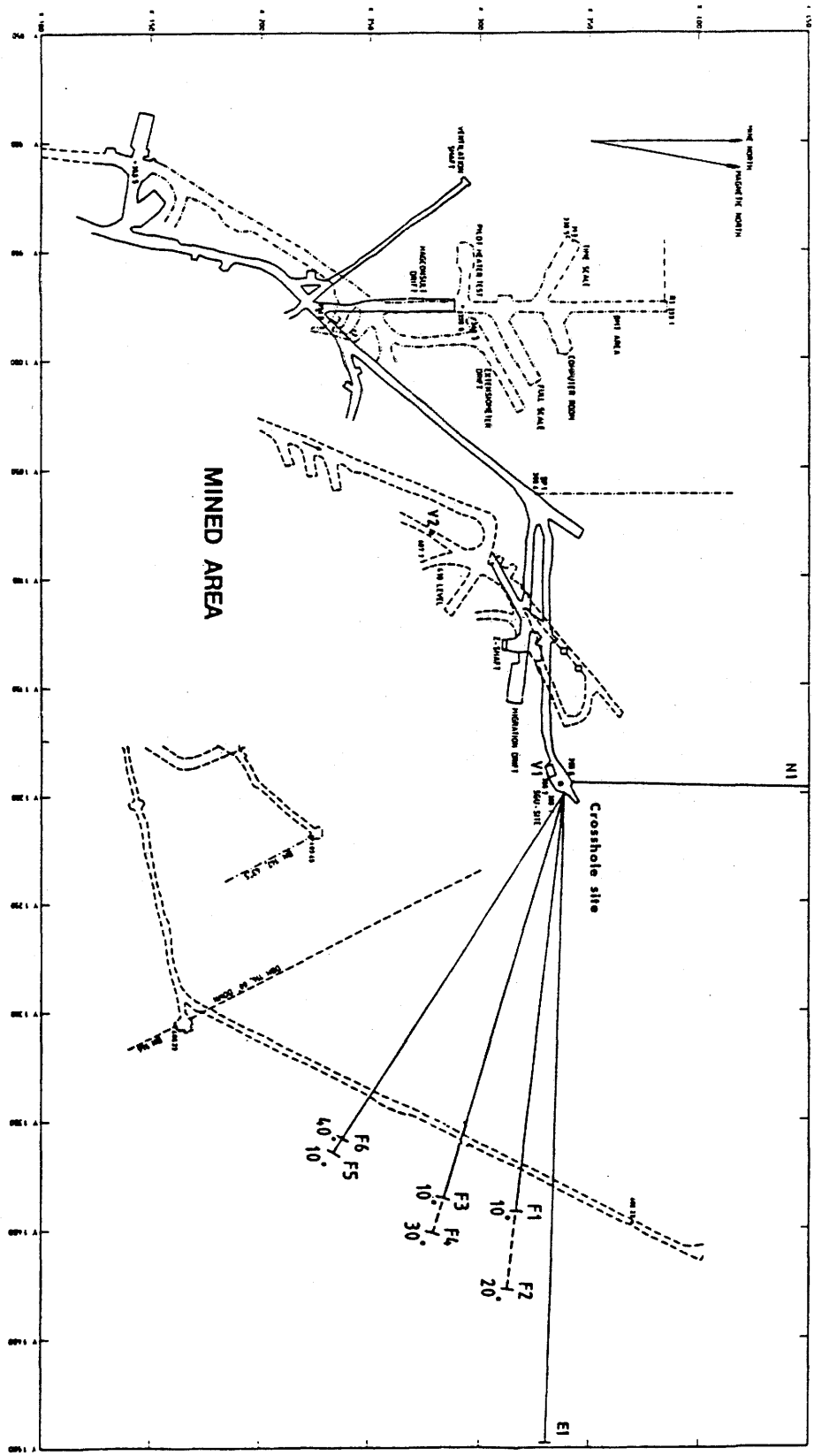


Figure 1-1 Map of the Stripa mine at 360 m level. Boreholes F1-F6.

# 2 REFLECTION ANALYSIS

## 2.1 INTRODUCTION

The original crosshole seismic measurements were performed on five sections between 60 m and 200 m depth in the boreholes F1 to F6. Two series were recorded for each section, with the ray net shifted by 5 m between the series. For each series, the distance between subsequent measuring and receiving positions was 10 m. In addition, part of the section between boreholes F4 and F6 was sampled with a more dense ray coverage. Here the source and the detector spacing was 2.5 m.

It should be born in mind that measurements which are intended for tomographic analysis have to be made with a large number of source and detector positions in each borehole. The main concern is to get a uniform ray-coverage and it is not necessary to record at all receiver positions for each source position. Usually one omits such source/detector combinations where the source and the detector are at opposite ends of the section, as the corresponding long rays do not contribute very much to the tomographic analysis.

The reflection analysis is different in the sense that it is applied to sets (profiles, common-shot gathers) of seismograms recorded at all possible detector positions with the source in a single location. The records are then stacked, i.e. added, in a special way to enhance the desired reflections. If the waves from a single source position are recorded at a few detector positions only, the corresponding profile will be too sparse.

Another difference is that the detector spacing must be shorter for reflection analysis than for tomography. It must be possible to follow the same reflected phase from trace to trace. If the time difference between two adjacent traces is more than half a period, it becomes difficult to decide which onsets that correspond to the same event.

One could say that the profile is sampled in two dimensions, space and time. In order to avoid aliasing, the sampling interval in the spatial domain (the detector spacing S) must be smaller than one half of the shortest signal wavelength (LAMBDA). This relation can be expressed also in terms of vave velocity (V) and maximum signal frequency (FMAX):

$$S < LAMBDA / 2 = V / (2 * FMAX)$$

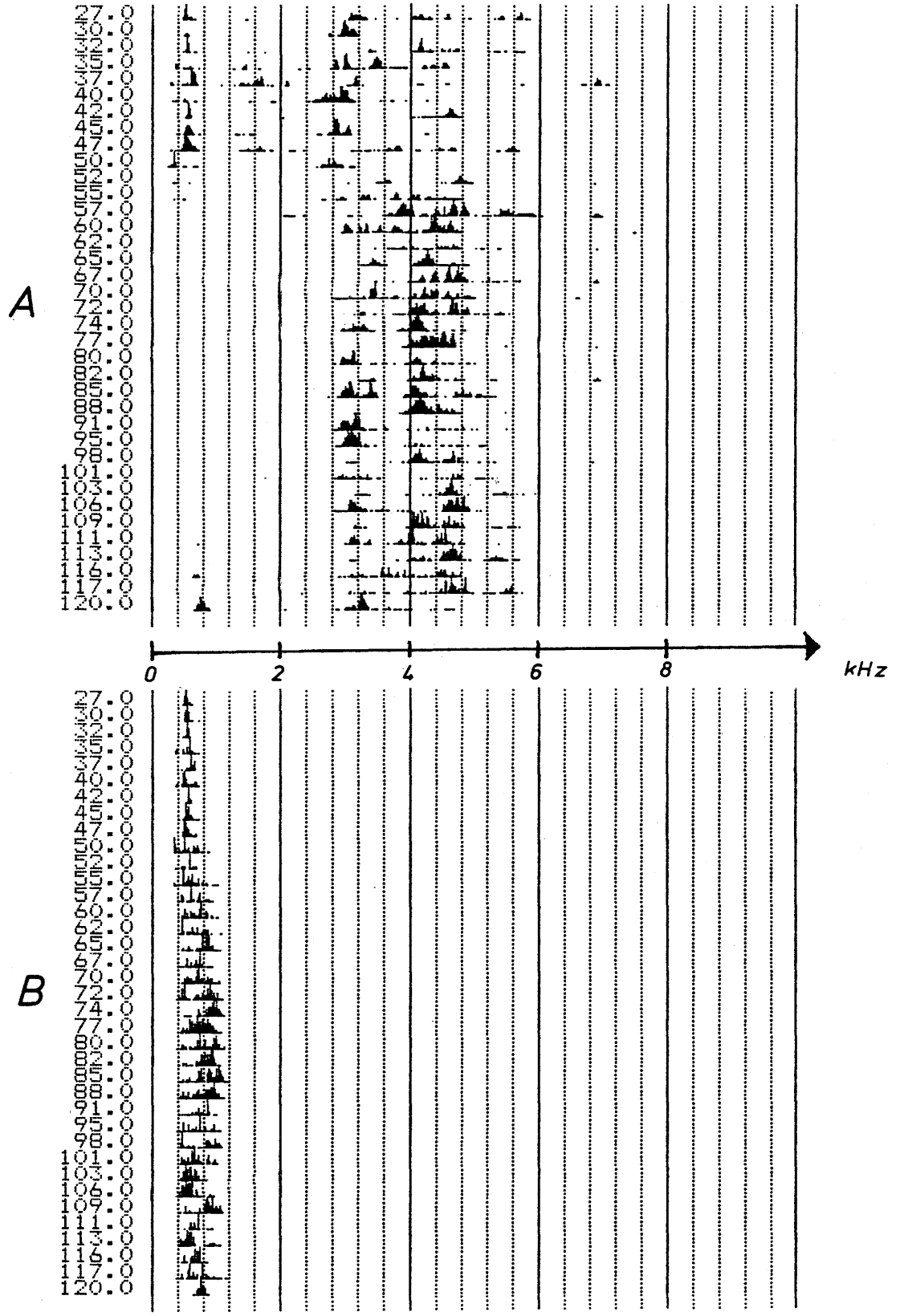


Figure 2-1 A. Example of amplitude spectra. For most traces the frequencies below 1 kHz are not visible with this plot scale.
B. Spectra of the same profile after filtering (400-1000 Hz) and rescaling.

A too large detector step would either produce spatial aliasing or limit the usable frequencies too much. For a detector spacing of 5 m the frequency limit is around 500 Hz. In the recorded signals very little energy is present below this frequency, which makes the analysis difficult (Figure 2-1).

The upper part of section F4-F6 was recorded with a denser spacing (2.5 m) and was consequently more suitable for reflection analysis. Data were available from 38 detector positions between 27 m and 120 m depth in borehole F6 with 10 source positions between 30 m and 75 m depth in F4. The Z-components (i.e., along the borehole), which contained most of the reflection information, were chosen for further processing.

For the reasons stated above, data from the other sections could not be used for reflection analysis.

## 2.2 EXPERIMENTAL TECHNIQUES

Seismic signals were produced at various depths by means of a steel hammer which could slide along the borehole inside a waterproof cylindrical enclosure. The trigger signal for the seismograph was picked up by a pulse sensor placed on a subassembly of the instrument which was rigidly clamped in the borehole (2).

Both P- and S-waves were generated by this device. The maximum S-wave output was obtained in the transverse direction. The unit was equipped with a hammer of 2.5 kg weight capable of delivering an output of 50 J per blow.

In order to reduce the background noise, a number of shots were made with the source and the detectors at the same positions. The recorded signals were stacked (i.e., added) directly in the field. The number of measurements added for the same record varied between 5 and 20.

The detectors consisted of three accelerometers (100 mV/g) deployed at right angles, preamplifiers (40 dB or 60 dB) and a borehole clamping mechanism actuated by an electric motor.

In the picking of arrivals for tomographic analysis, frequencies up to 10 kHz had been used. The linear response required for reflection analysis limited the the usable frequencies to 3-5 kHz.

## 2.3 PROCESSING OF CROSSHOLE REFLECTION DATA

### 2.3.1 Amplitude Compensation

Normalization had to be done in order to cancel the effects of geometrical spreading and attenuation, which make raw signals from distant sources much weaker than those from close ones.

TAR (True Amplitude Recovery) is a variable gain operator which was run along the signal to increase the amplitude of later events, which are assumed to have travelled along longer paths. Considering geometrical spreading only, the samples of each trace could naturally be multiplied with (t/to) where 't' is the current time of the sample and '$t_o$' is the arrival time of the direct P-wave. We have used this factor raised to the power 1.15 to compensate for nonelastic attenuation and also for losses at reflecting interfaces.

### 2.3.2 Frequency Filtering

Most of the energy in the seismograms was concentrated between 6 and 10 kHz (Figure 2-1). However, we had to filter away the frequencies above 1 kHz to avoid spatial aliasing. The background noise at the lower end of the spectrum was filtered away by a low-cut at 400 Hz.

The original intention when the data was recorded was to get high frequencies to enable the accurate determination of traveltimes for tomographic processing. The high-cut at 1 kHz used in this study left little real signal energy in the seismograms and the dynamic range of the records became very poor.

### 2.3.3 Deconvolution

The source signal which is actually transfered to the rock is not a clean, single pulse. The high local stresses near the source and the coupling to the borehole change the original pulse shape. This causes problems in the interpretation. Reflections which arrive just after the direct P-wave are difficult or impossible to see. Multiple reflections involving both sides of a fractured zone can also create disturbing reverberations. Effects of this kind can in principle be eliminated by deconvolution.

We have tried two types of Wiener-filtering : prediction-error deconvolution and least-squares inverse filtering. In inverse filtering we try to change the original pulse (**P**) into a shorter wavelet (**W**) by using a filter operator (**F**), which will minimize the error

between the calculated wavelet (**F*P**, an asterisk stands for convolution) and the desired wavelet (**W**). Here (**W**) was chosen to be the first part of the original pulse (**P**). Prediction-error deconvolution multiple effects, which can be predicted from knowledge of the traveltime of a primary reflection. If we know the original pulse (**P**), or more precisely its autocorrelation function, we can construct a filter operator (**F**) which - when applied to the whole signal (**S**) - predicts the later arriving parts of (**S**). Thus the difference (**S-F*S**) does does not contain the multiples, few, non-predictable cycles of (**S**).

The result of our analysis was that the deconvolution did not bring much improvement to individual traces. The source signals show practically no reverberations in the low-frequency band. When looking at the entire profile, the deconvolution had an effect of focusing and the reflection patterns generally became clearer.

### 2.3.4 Coherency Stack

If the seismic velocities are fairly constant and the reflectors are flat over a distance of a few wavelengths, the pattern of the reflected events in the profiles can be calculated geometrically. Reflections from a known boundary can be enhanced in principle by shifting each trace by an appropriate traveltime. However, the two-way travel time shift, which is a common procedure for surface reflection surveys in layered media, can not be applied with the crosshole geometry in crystalline rock. The reason is that with crosshole reflection surveys the source and the receivers are always placed in different holes, i.e. the source is always laterally offset with respect to the array of detectors. Moreover, in crystalline bedrock the reflectors may have any dip and strike.

In general, the events identified in the profiles will show up as hyperbolas with occasional deviations due to velocity variations. It is possible to enhance coherent reflections by stacking, i.e., by adding together a few adjacent traces along the travel time hyperbola corresponding to the assumed inclination and depth of the reflector. The results can be further improved if the stacked trace is multiplied by some coherency function, for example by the semblance operator of the original traces. In the ideal case the section of traces obtained in this way contains reflections from boundaries which observe a certain relation between dip and strike (see section 2.4).

It must be pointed out that due to spatial aliasing, stacking may also enhance events which are not reflections. The tubewaves are the most disturbing events due to their low velocity (appr. 1400 m/s, see sect. 3.2.2). The frequency range used in this study (400 Hz - 1000 Hz) gives wavelengths of 1.5 m - 4 m for the tubewaves. One can see in Figures 4-1 to 4-5 that the average tubewave frequency is close to 1000 Hz and therefore a considerable amount of tubewave energy will be aliased in the stacking process.

It seems that aliased energy can be suppressed by averaging over several stacked sections. When stacking is made with all reasonable values of dip and strike and the resulting sections are added together, we get a section where reflections with different angles are clear, but where the aliased tubewaves have been partly removed in the process. Three examples of processed profiles are shown in Figures 2-2 A, 2-3 A and 2-4 A.

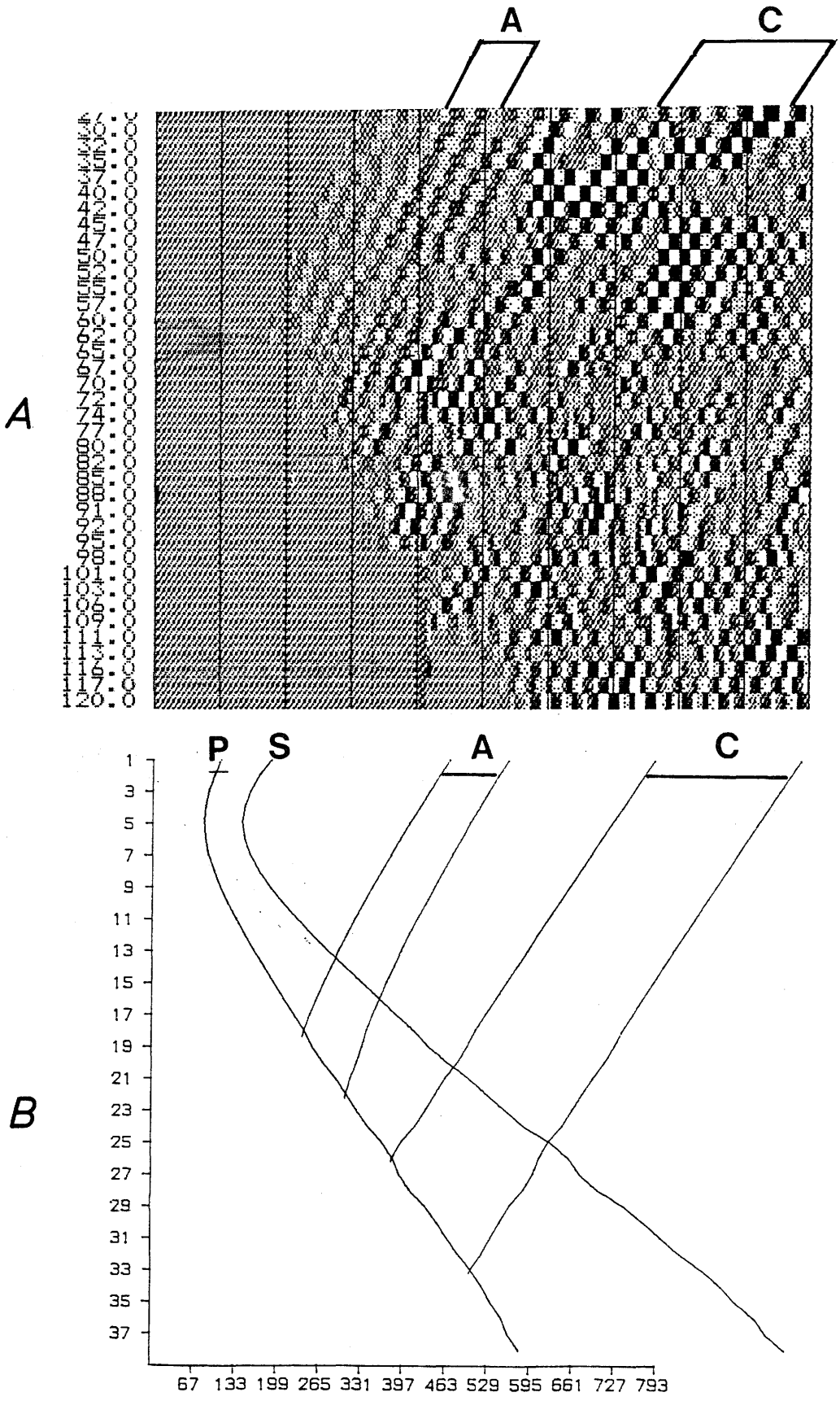


Figure 2-2 A. Processed profile (F6) with source at depth 40 m in F4. Zone "A" at 70-77 m. A boundary of zone "C" at 95 m. The other side of zone "C" is less clear.
B. Synthetic travel times for the reflectors above. 'P' and 'S' are the direct arrivals of the compressional and shear waves.

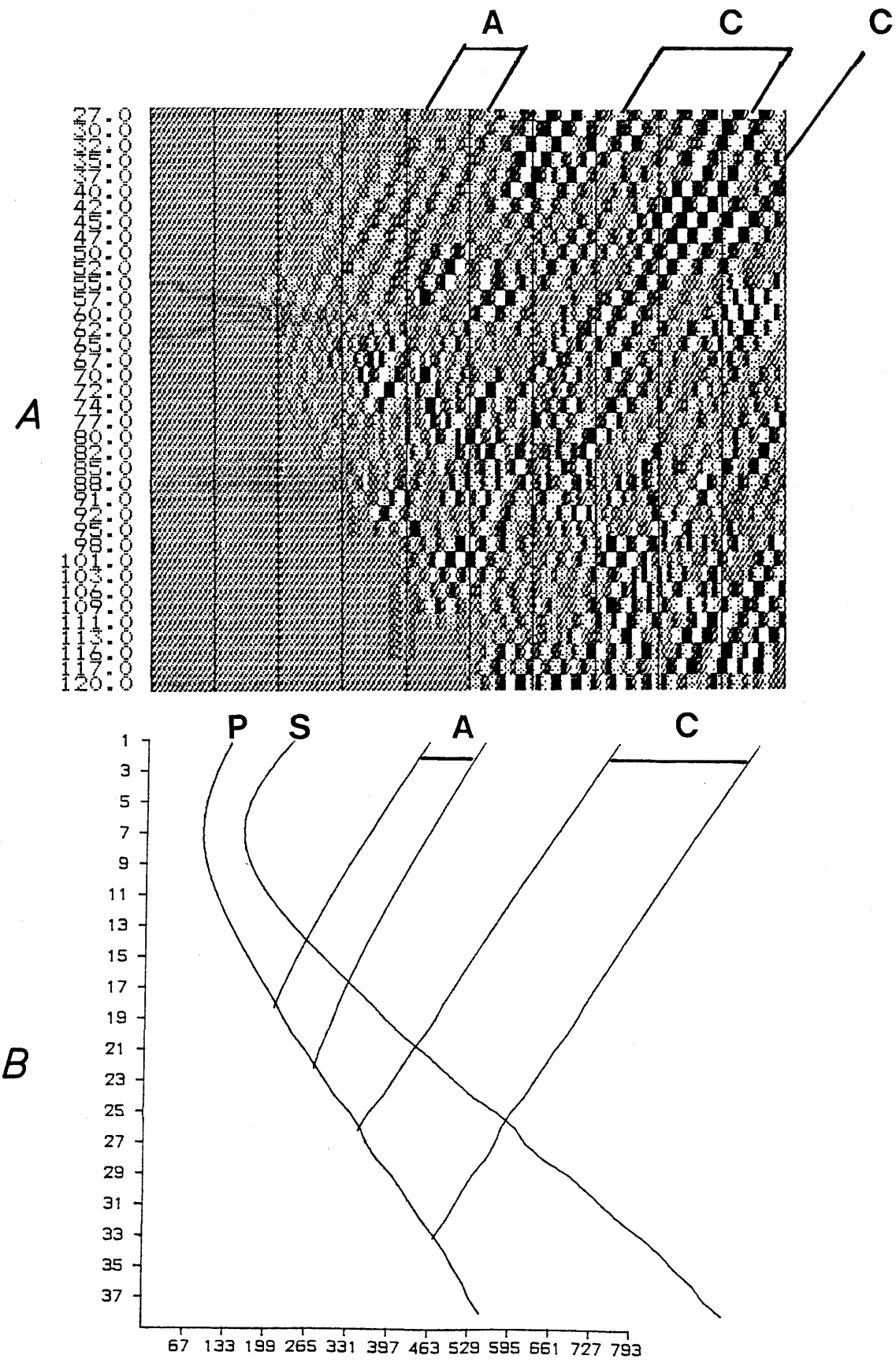


Figure 2-3 A. Processed profile (F6) with source at depth depth 45 m in F4. Zone "A" is weak. The lower edge of zone "C" (110 m) stands out clearly. Another event ("C'") can be noticed just below zone "C".
B. Synthetic travel times for zones "A" and "C".

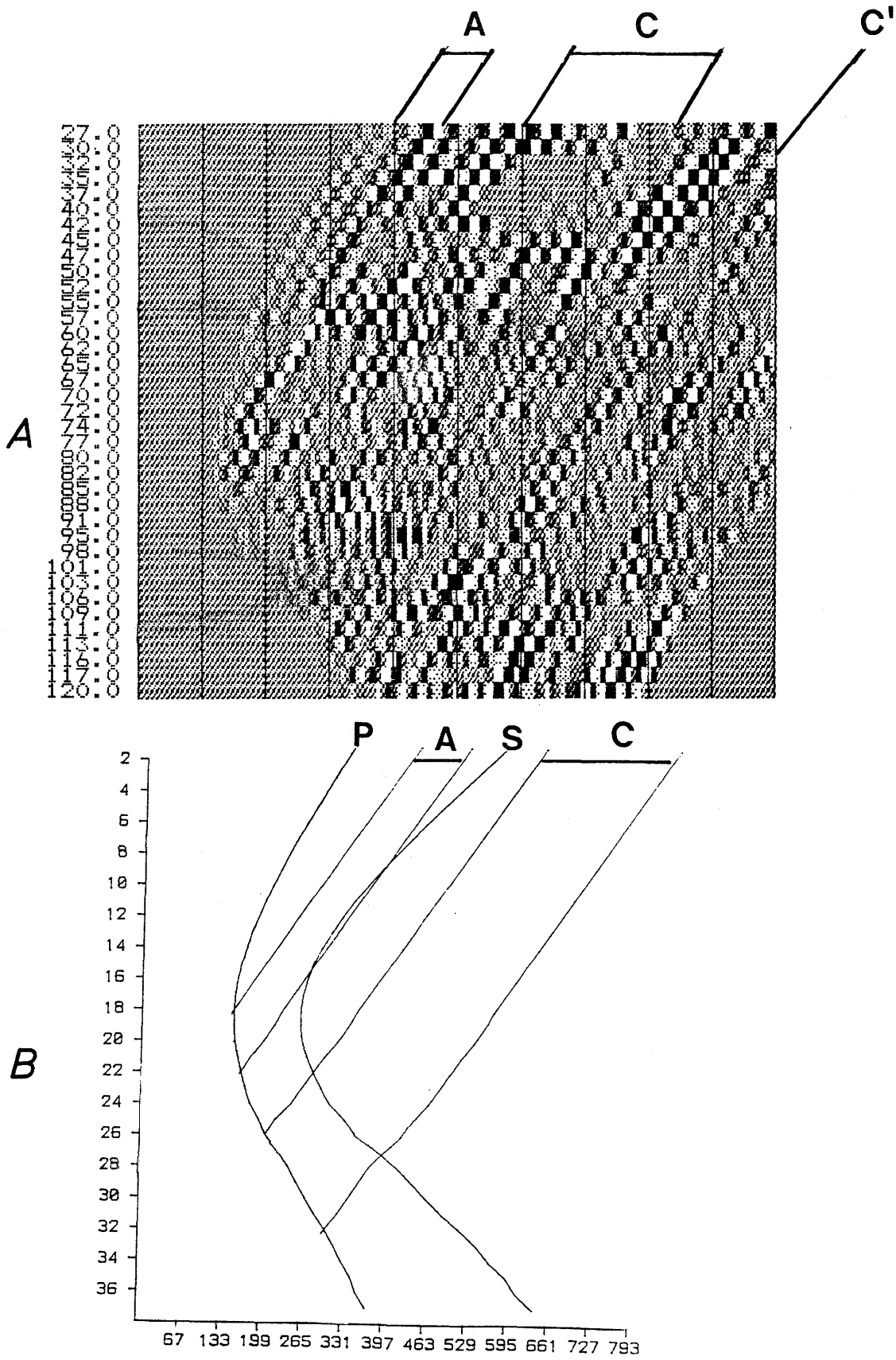


Figure 2-4 A. Processed profile (F6) from a deeper source (75 m) in F4. Zones "A", "C" and one edge of "C'" are pointed out. Deeper reflectors can be noticed. The direct S arrivals induce disturbances.
B. Synthetic travel times for zones "A" and "C" in the profile above.

## 2.4 3-D ORIENTATION OF THE REFLECTORS

Neither the dip nor the strike of a reflector can be determined independently from only one profile. The traveltime for the reflection from a given plane reflector is:

$$t(Z) = \mathrm{SQRT}(X^{**}2 + 4*D*(D-Z) * h * \cos(\mathrm{THETA}) + Z^{**}2) / v$$

where

$$h = \cos(\mathrm{THETA}) * (1 - X/D * \tan(\mathrm{THETA}) * \cos(\mathrm{PHI}),$$

THETA is the dip of the reflector,
PHI is the declination of the reflector,
X is the distance from the source to the borehole,
D is the depth of the reflector in the hole,
Z is the depth of the receiver in the hole,
v is the average wave velocity.

For the definition of parameters see also Figure 2-5 A. The unknown parameters D and ( h * cos(THETA) ) can be calculated from the observed hyperbolic patterns formed by the traveltimes in the section of seismograms. It can be seen that the traveltime will remain unchanged, even if the dip and strike change, as long as ( h * cos(THETA) ) is constant. The allowed values for dip and strike ( for h * cos(THETA) = const.) will define a curve like those in Figure 2-7. To get a unique solution for dip and strike, the same reflector must be found in at least three profiles with different source positions.

The same conclusion is reached by following a geometrical reasoning. With a reflector of arbitrary dip and strike crossing the detector borehole at D (Figure 2-5 B), all possible images of the source S can be found on a sphere of radius DS. However, the distances from images located on the same latitude circle (e.g., I1 and I2) to the same detector X are equal. Assuming that the wave velocity is constant, one gets the same reflection pattern from any of these images. Therefore, the reflector position can not be determined from its trace in a single profile but, according to the condition imposed, it must be tangent to a defined conic surface which intersects the plane of Figure 2-5 along 'Ref 1' and 'Ref 2'.

If the same reflection pattern can be recognized in the profile obtained from a different source position, the same considerations will lead to the definition of another conic surface. The reflector can then occupy only the two positions in which it is tangent to both cones and a third profile can decide which of them is the actual one.

For the actual determination of the reflector position, a corresponding reflection event must first be found in

the profiles. Synthetic curves are then drawn on a graph for different possible dips of the reflector (Figure 2-6). The curve which matches the actual reflection pattern best will give the relative dip of the reflector with respect to the specific profile (Figures 2-2 B, 2-3 B and 2-4 B).

The reflectors at zone "C" can be seen as a set of parallel events. The main ones appear at approximately 95 m and 110 m depth. The depth determination is approximative because of the low frequencies that we had to use. The matching curves could just as well be translated half of a wavelength towards positive or negative times. This corresponds to an error of 5 m in the location of the reflector.

It could be inferred (e.g., from Figure 2-3 A) that another reflector with a slightly different orientation crosses F6 at 10 m further down. However, the low-resolution areas of the plot, which were occupied before processing by tubewaves, do not permit a clear identification of the intersection point. Zone "A" also appears in the plots, although it is weaker than zone "C".

Each relative dip corresponds to a conic surface (Figure 2-5) and expresses a relation between the actual dip and strike. This relation can be represented as a curve in a Wulff diagram like the one in Figure 2-7. The intersection of more curves would give the actual dip and strike.

When all the sources belong to the same crosshole section as in this case, the best estimate for the dip and strike will be given by the curve with the smallest area. In principle, if the image source corresponding to a certain relative inclination lies along the detector borehole, the dip and strike of the plane will be uniquely determined.

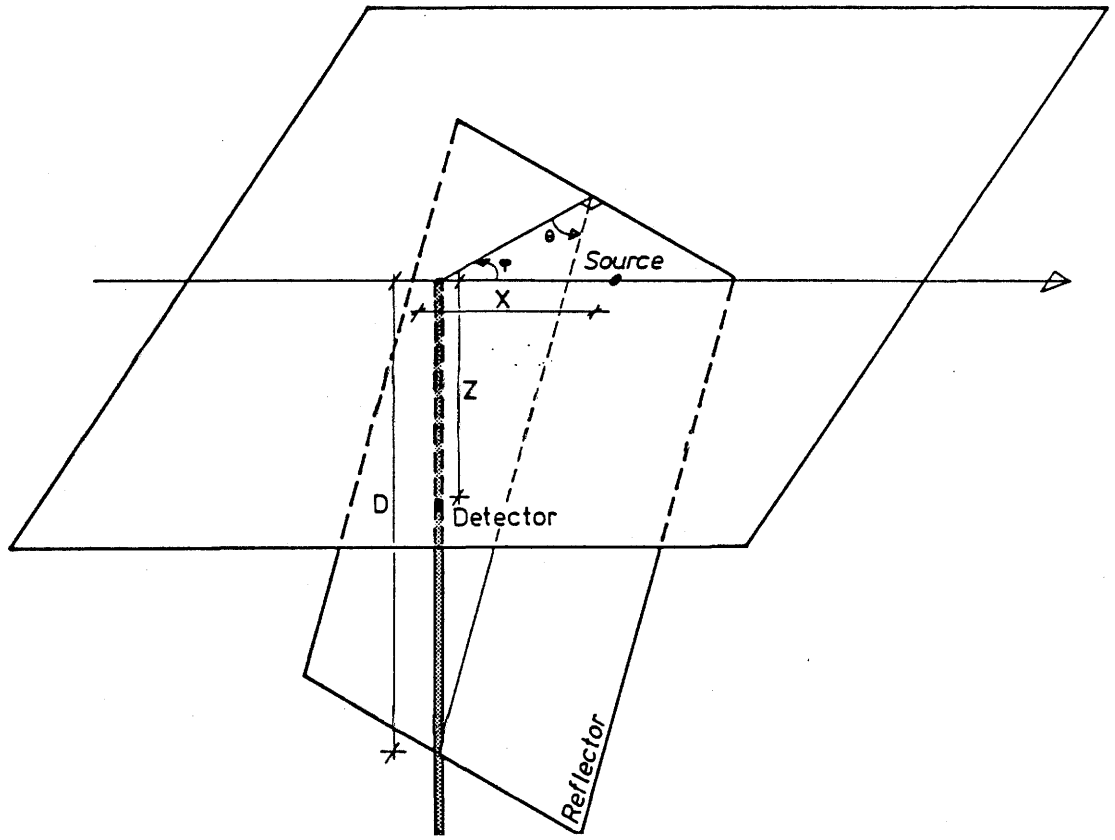


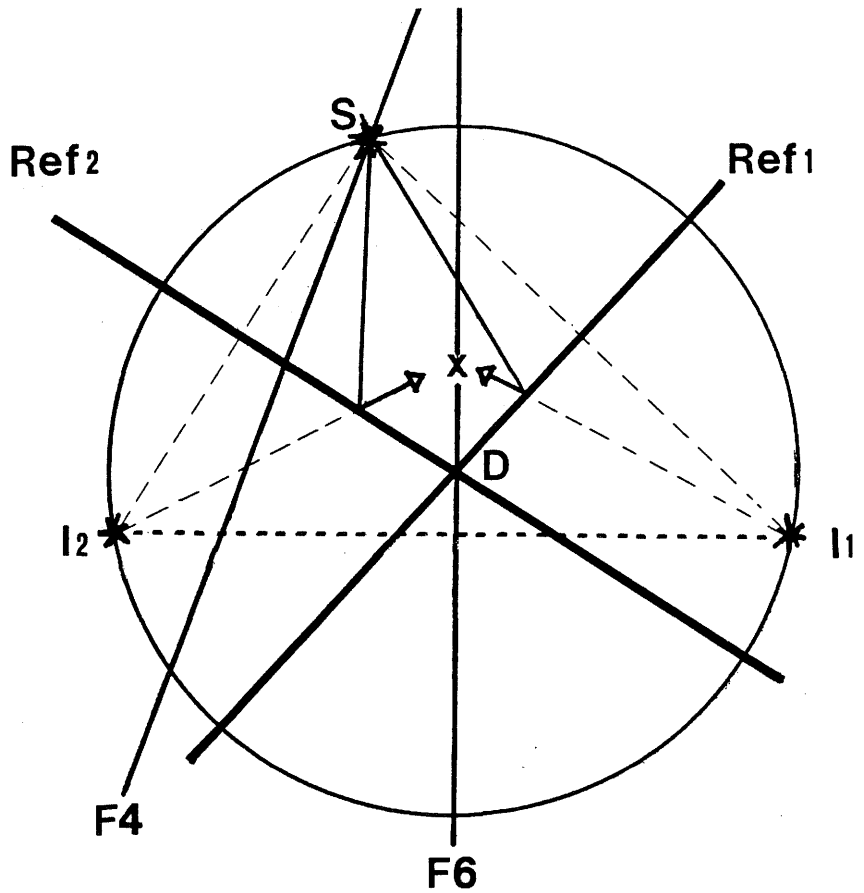


Figure 2-5 A. 3-D orientation of a reflector.
B. The positions Ref 1 and Ref 2 generate the same pattern (I1 and I2 are equidistant). If the image lies at one poles of the sphere the position is fixed from only one profile.

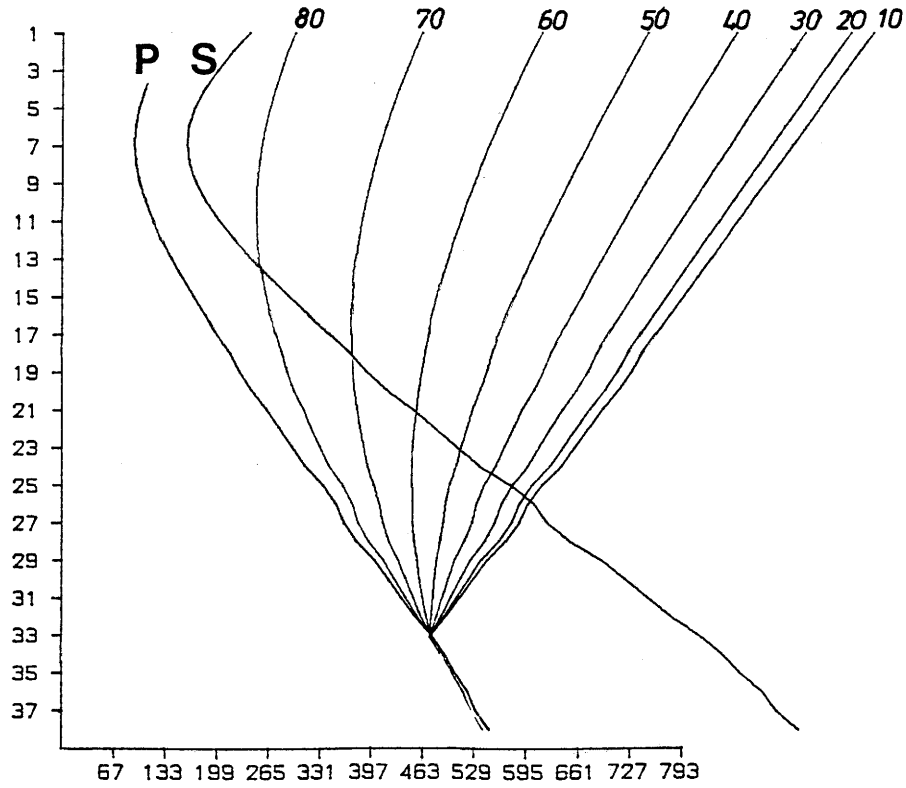


Figure 2-6 Synthetic arrivals for several relative inclinations. The best fitting value is chosen by comparison with the reflections identified in the corresponding profile. Large relative inclinations can be determined with higher accuracy.

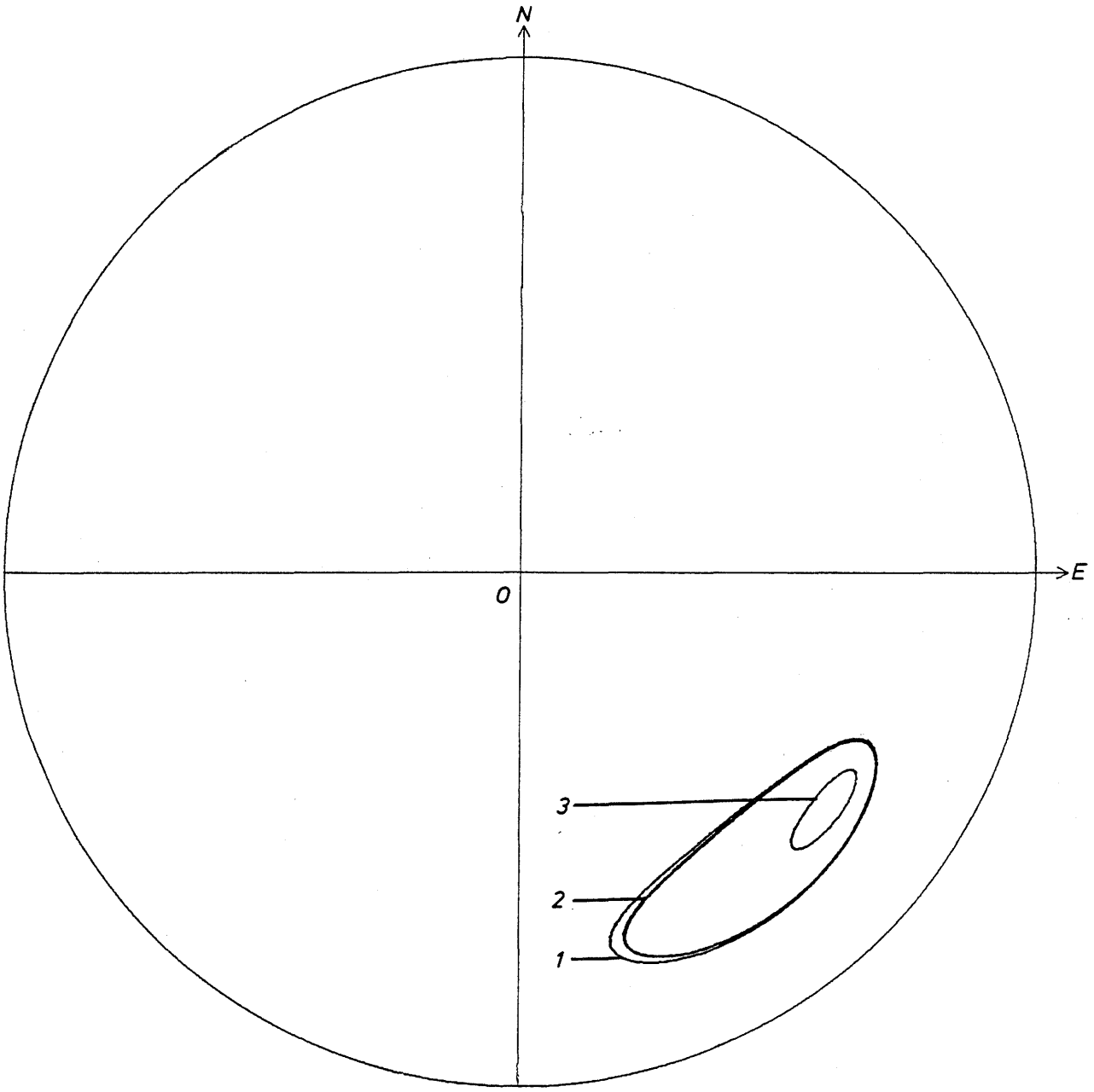


Figure 2-7 Wulff diagram (downgoing normal) showing the 3-D orientation of zone "C" calculated from the profiles in figures 2.2 - 2.4. Source depth: 1: 40 m, 2: 45 m, 3: 75 m.

## 2.5 COMPARISON WITH EXISTING MODEL

The reflection analysis of crosshole seismic data reveals a main zone "C" crossing the borehole F6 at 95 m and at 110 m. Calculations with the source at 75 m give a dip of 65 to 71 degrees and a strike varying between 225 and 235 degrees, see Figure 2-7.

Previous investigations placed zone "C" between 95 m and 118 m depth with the exception of the single-hole hydraulic tests which placed it between 115 m and 132 m. It is possible that hydraulics refer to a deeper part of zone "C" which is also indicated by seismics.

In the radar measurements (5) zone "C" is placed at 103 m (60 MHz radar) and 118 m (20 MHz radar). The 103 m estimate probably represents the feature described above. The differences in depth determinations are due to experimental errors and the fact that the boundaries "seen" in each case are not the same. The radar reflections occur at discontinuities for the electrical conductivity, while seismic reflections occur at steep changes of mechanical properties. The orientation of zone "C" calculated by 60 MHz radar is: dip 73 degrees and strike 223 degrees. This is in very good concordance with the seismic results. The difference of a few degrees is not important since the fractured zones are not expected to be exactly planar.

# 3 TUBEWAVE ANALYSIS

## 3.1 INTRODUCTION

Tubewaves are low velocity, large amplitude seismic waves (of the Stonely wave type) which propagate along the interface between the borehole wall and the borehole fluid. They are generated by the interaction between a compressional wave in the surrounding rock and discontinuities in the borehole. The compressional wave forces the water at the discontinuity into the borehole, where conversion to tubewaves takes place. Mapping these "conversion zones" makes it possible to detect hydraulically conductive zones in the rock.

Tubewave analysis has been performed on crosshole seismic data from the sections between boreholes F1-F6. Seismic signals were generated in the borehole F4 and recorded in the holes F2, F3, F5 and F6 between 60 and 200 m depths. (Details on the experimental technique were given in chapter 2.2 above.)

Measurements were also performed between the boreholes F5 and F6 and differ from those described above. Explosive charges up to 5 g were set off in borehole F5 and recorded in F6. The shot depths were between 34 m and 200 m and the recording depths between 45 m and 250 m. (A detailed technical description is given in (4).

Signals produced from two kinds of sources, mechanical ones and explosives, were recorded by three-unit accelerometer chains, each unit consisting of three components, two which are radial along borehole axis (X and Y) and one (Z) parallel to it. The Z-components yielded the best response for tubewave phases and were chosen for further processing and analysis.

The most common shot/receiver configuration used for tubewave analysis is the VSP (vertical seismic profiling) geometry. In the VSP method, signals are generated at the same location and recorded at successively increasing (or decreasing) depths. If tubewaves exist, they can be followed over a number of traces.

Unfortunately only a few recordings for each source position were available. (This was sufficient for the tomographic analysis for which the data were primarily intended.)

## 3.2 TUBEWAVE PROCESSING PROCEDURES

### 3.2.1 Filtering

The recorded signals were divided into groups containing traces from the same source position (3-7 traces per source position). Spectral analysis was used in order to improve the signal-to-noise ratio and to enhance signals with frequencies corresponding to tubewaves. It was found that most of the energy originating from tubewaves was concentrated to frequencies between 1 and 2 kHz.

### 3.2.2 Velocity and Amplitude Estimations

Onset times for the tubewaves were picked and the velocity was found to be 1410 m/s, with an error bound of 10 m/s. Examples of signals containing tubewave phases are given in Figures 4-1 to 4-5. The velocity of the surrounding rock as determined from the tomographic analysis (4), was 6000 m/s. The amplitudes were measured by integration over the tubewave wavelets and corrected for differences in source/receiver distance.

### 3.2.3 Location of Tubewave Sources

Since the boreholes F1-F6 are not parallel some geometric calculations had to be performed for determining the depths of the discontinuities generating tubewaves. A computer program which calculates these depths was written. The input parameters are the angle between the boreholes, the source depth, the receiver depth, the onset time for the tubewave, the tubewave velocity and the P-wave velocity (Figure 4-6).

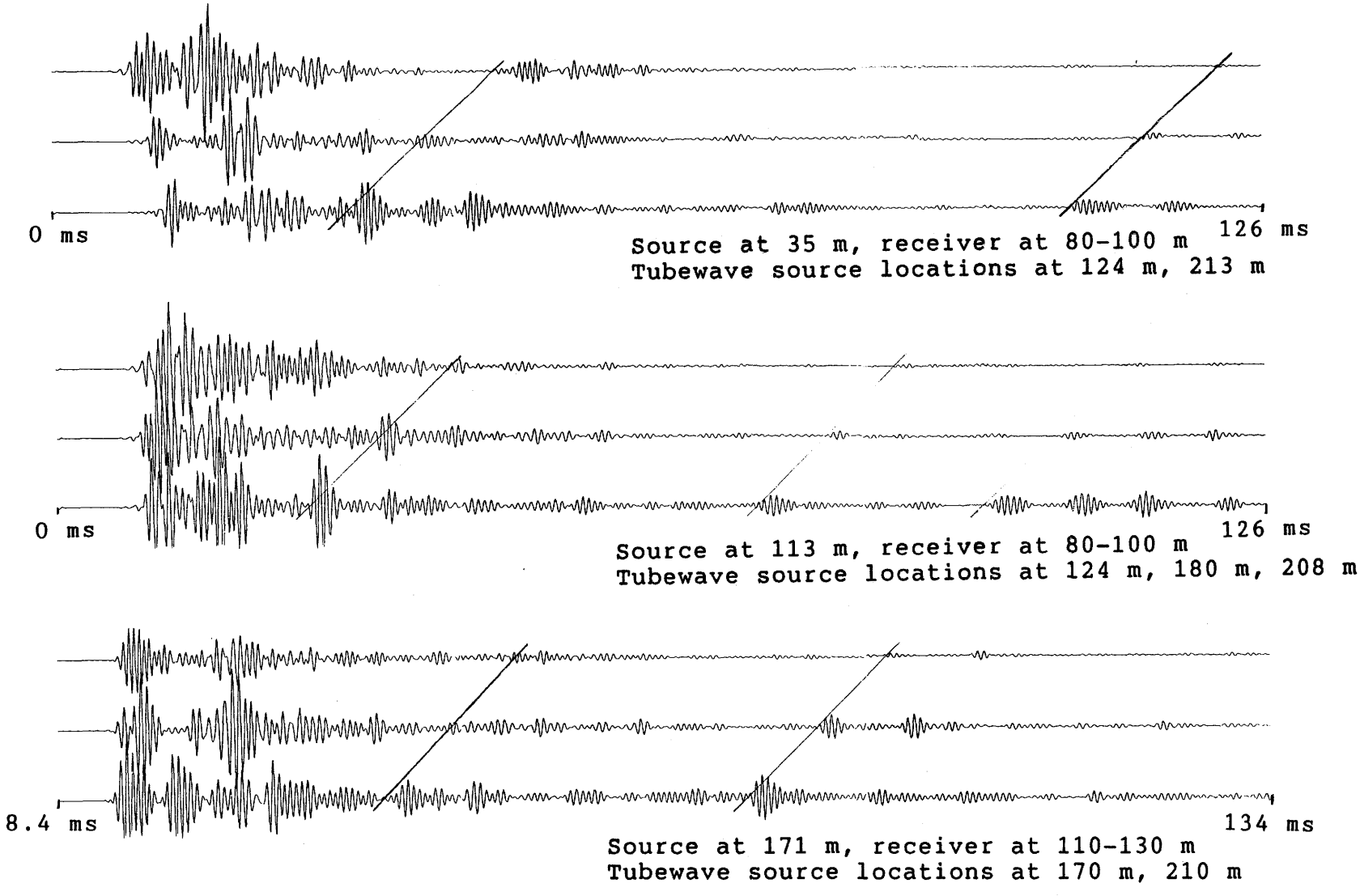


Figure 4-1 Seismic registrations from different source and receiver depths. Tubewave onsets are connected by straight lines. Seismic source in F5, receivers in F6.

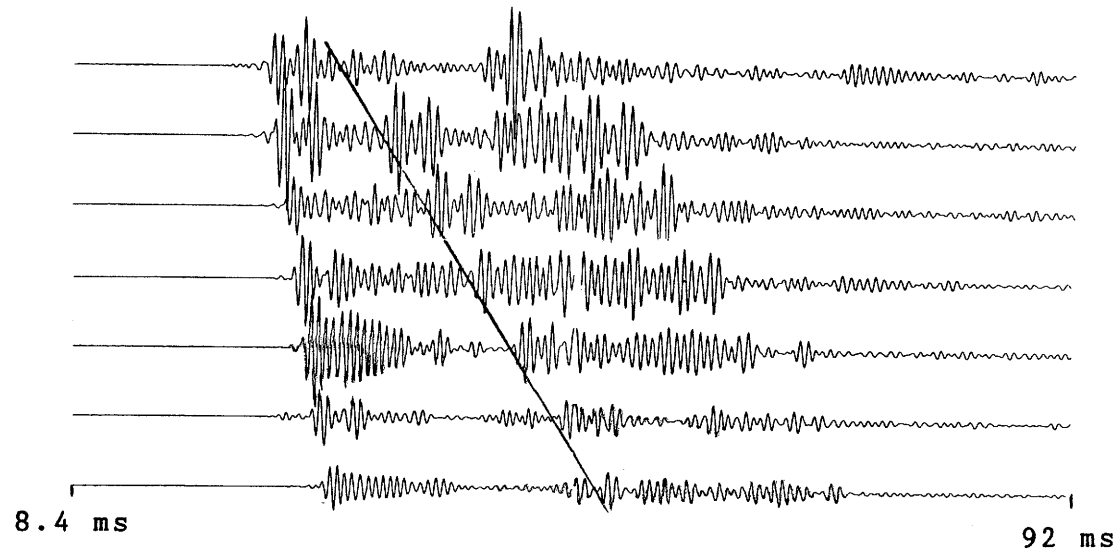


Source at 90 m, receiver at 220-250 m
Tubewave source location at 215 m

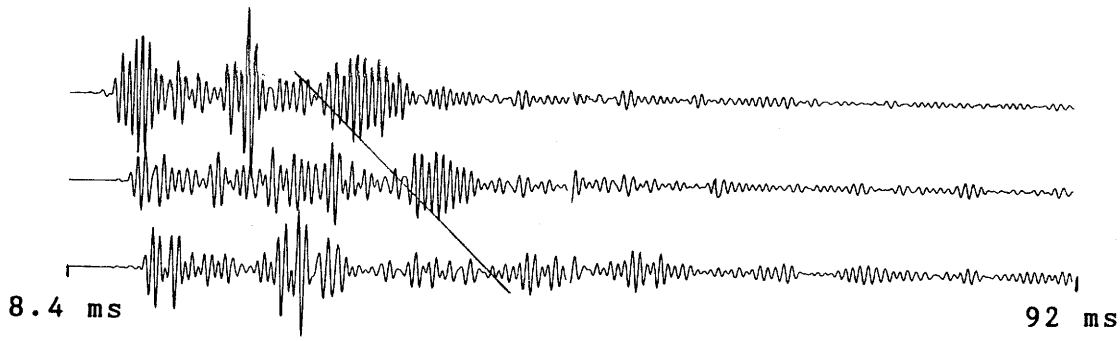


Source at 92.5 m, receiver at 140-160 m
Tubewave source location at 117 m

Figure 4-2 Seismic registrations from different source and receiver depths. Tubewave onsets are connected by straight lines. Seismic source in F5, receivers in F6.

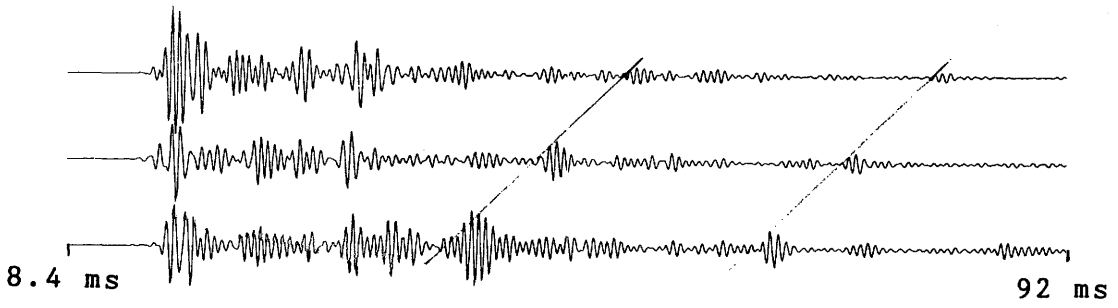


Source at 195 m, receiver at 165-185 m
Tubewave source locations at 223 m, bottom of the hole

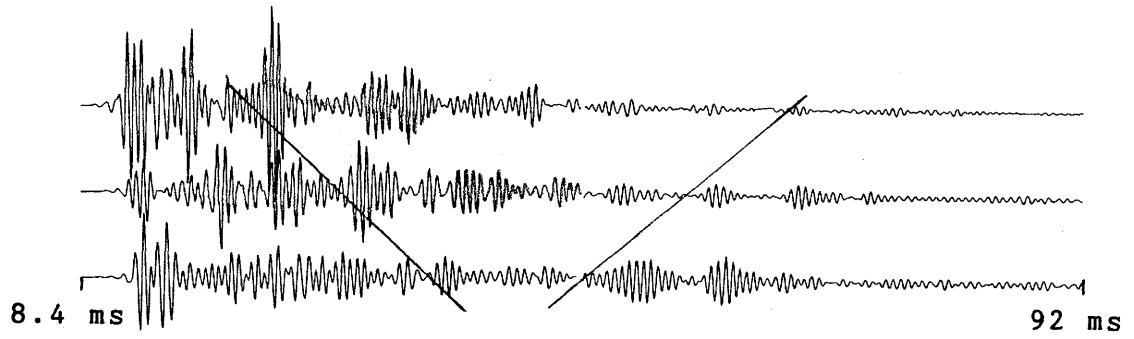


Source at 140 m, receiver at 140-160 m
Tubewave source locations at 122 m, 213 m

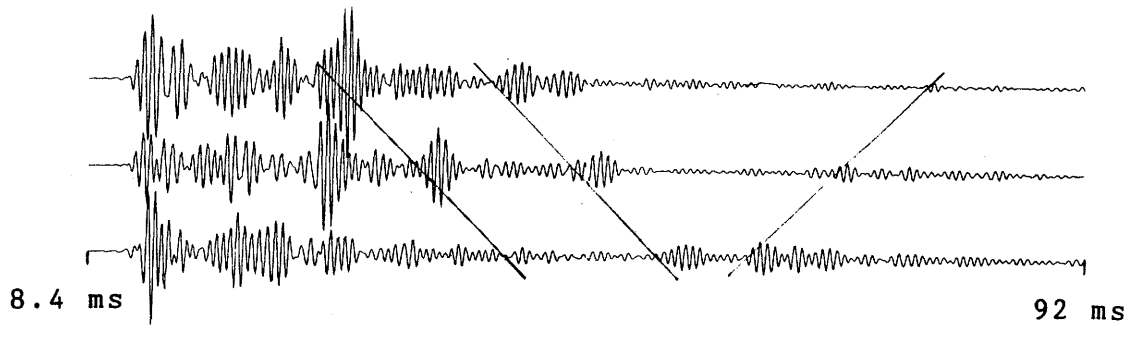


Source at 146 m, receiver at 135-155 m
Tubewave source locations at 112 m, 52 m, 222 m

Figure 4-3 Seismic registrations from different source and receiver depths. Tubewave onsets are connected by straight lines. Seismic source in F5, receivers in F6.

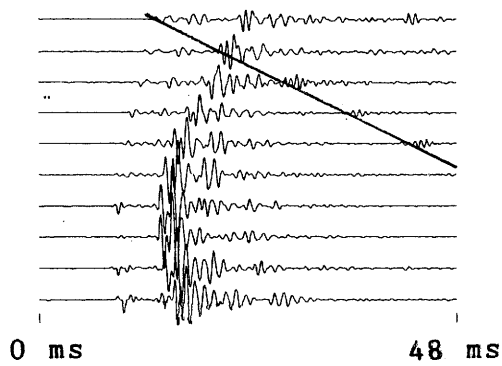


Source at 125 m, receiver at 180-90 m in F1
Tubewave source location at 185 m

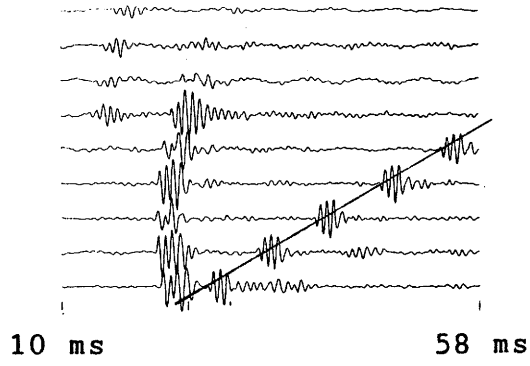


Source at 189 m, receiver at 155.5-193.5 m in F1
Tubewave source location at 213 m

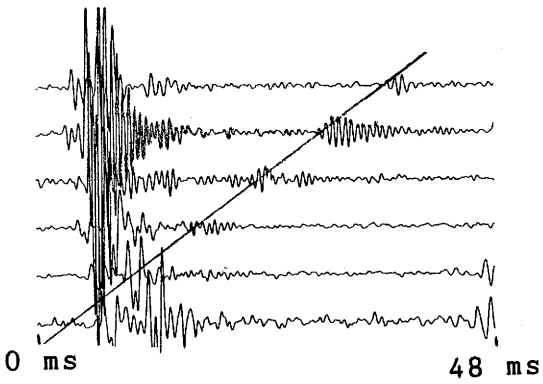


Source at 75 m, receiver at 60-110 m in F2
Tubewave source location at 106 m

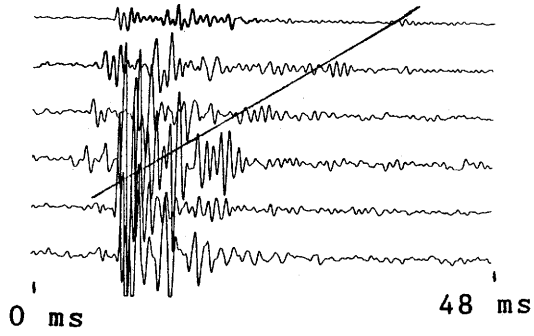


Source at 125 m, receiver at 80-130.5 m in F2
Tubewave source location at 123 m

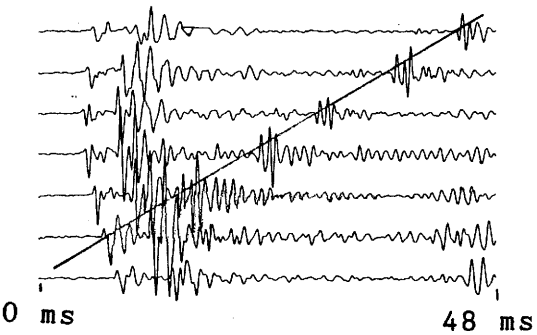


Source at 85 m, receiver at 60-120 m in F3
Tubewave source location at 115 m

Figure 4-4

Seismic registrations from different source and receiver depths. Tubewave onsets are connected by straight lines.

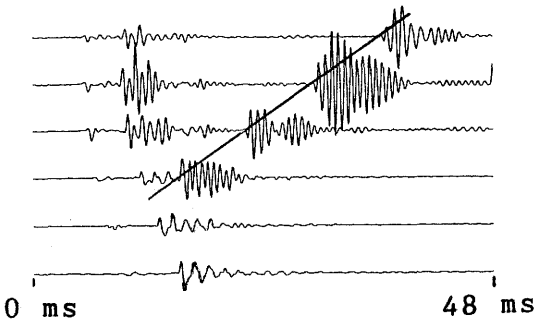


Source at 75 m, receiver
at 60-110 m in F5
Tubewave source location
at 104 m

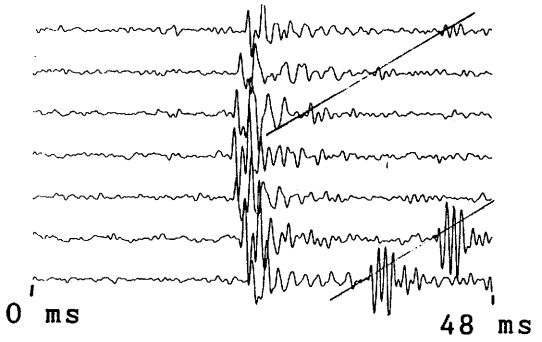


Source at 170 m, receiver
at 125-195 m in F5
Tubewave source location
at 155 m

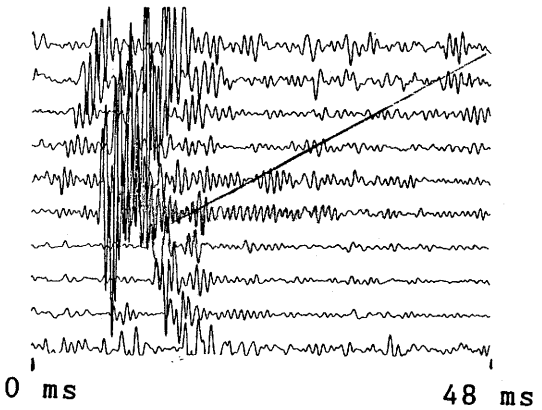


Source at 145 m, receiver
at 200-111.5 m in F6
Tubewave source location
at 134 m

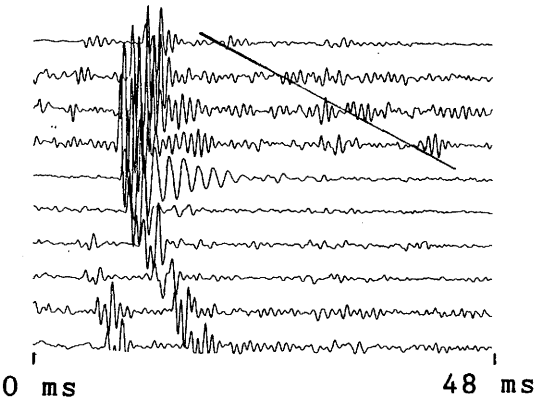


Source at 175 m, receiver
at 200-111.5 m in F6
Tubewave source location
at 221 m

Figure 4-5 Seismic registrations from different source and receiver depths. Tubewave onsets are connected by straight lines. Seismic source in F4.

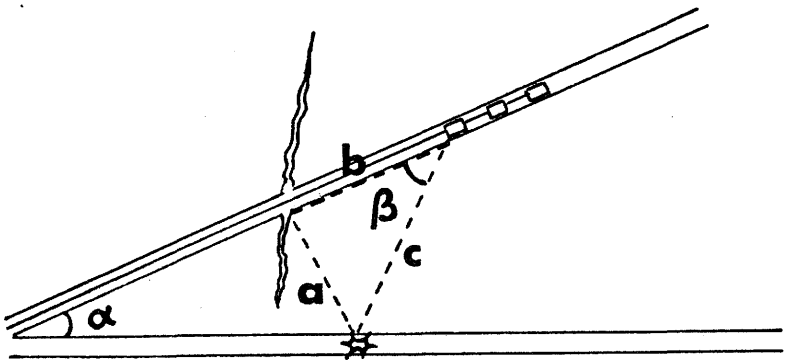


Figure 4-6 The geometrical relationship between seismic source, tubewave source and receivers.

## 3.3 COMPARISON WITH EXISTING MODEL

A comparison between tubewave analysis and hydraulic conductivity has been made for all boreholes except F4 (1). (F4 was only used as a source hole.) Figures 4-7 to 4-9 show relative amplitudes of tubewaves as a function of borehole depth and the corresponding hydraulic conductivity.

Our analysis has given the following results for the different boreholes:

**Borehole F1:**

Neither of the two tubewave sources correlate with single-hole hydraulic measurements (Figure 4-7), but both are visible with radar and seismic methods, (2,4,5). The source at 71 m is a local feature and the source at 180-181 m has been classified as zone "K".

**Borehole F2:**

Good correlation between hydraulic crosshole measurements and tubewaves is found around 100 m (Figure 4-7), which corresponds to the "C" zone. Singlehole hydraulic measurements indicate a conductive zone between 116-126 m. A few tubewaves originating from this interval are also found.

**Borehole F3:**

Zone "C" is clearly defined from tubewaves at 106-115 m (Figure 4-8). This depth was also obtained with hydraulic measurements, both single and crosshole.

**Borehole F5:**

Zone "C" is seen at 97-102 m (Figure 4-8) which correlates well with hydraulic singlehole measurements.

**Borehole F6:**

The tubewave analysis for borehole F6 was performed on recordings from both borehole F4 (mechanical source, Figure 4-9, upper part) and F5 (explosive source, Figure 4-9, lower part). For F5 a very scattered image of the tubewave sources is obtained. The amount of data for this section was larger than for the other sections. Identification of tubewaves was here in some cases difficult because of interfering seismic events of different origin. This is probably due to the relatively high variation in mechanical properties of the rock at this part of the measured volume. Looking at Figure 4-9, one can see a concentration of tubewaves originating from 112-130 m and from 208-230 m. Hydraulic single and crosshole measurements placed the zone "C" between 115-132 m, which is in agreement with tubewave source depths. The zone "L" was seen at 205-240 m by hydraulic singlehole measurements which also agrees with tubewave analysis.

Geometrical errors can cause differences between the "true" locations of the zones and those determined by tubewave analysis. One source of error is that borehole curvature was neglected when calculating tubewave source depths.(Figure 4-6). Another source of error is the determination of the tubewave onset times. Sometimes, the tubewave phases are obscured by other phases which makes time-picking difficult.

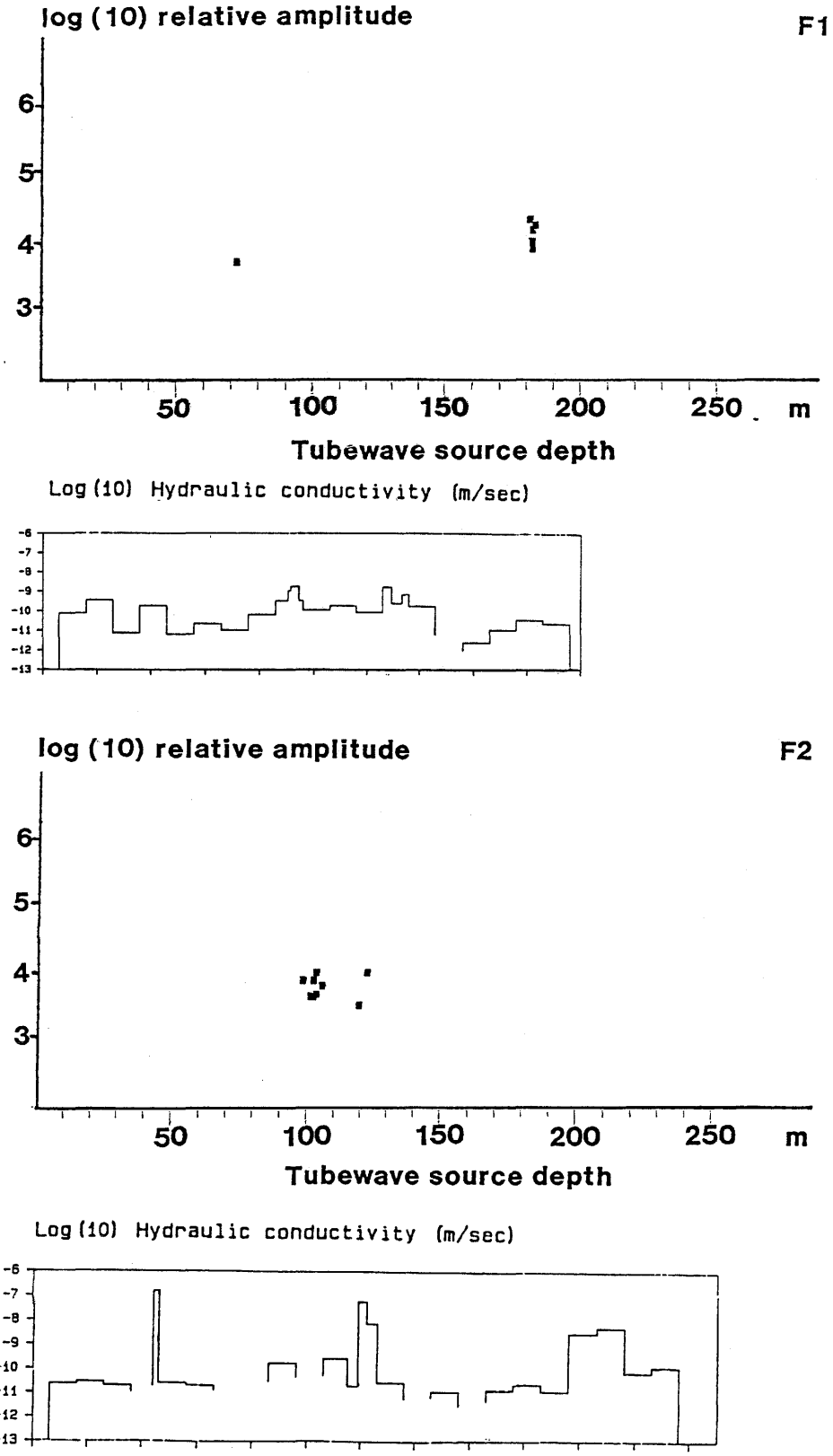


Figure 4-7 Tubewave relative amplitudes at different depths in F1 and F2 compared to hydraulic conductivity (1). Seismic source in F4, receiver in F1 (upper figure), receiver in F2 (lower figure).

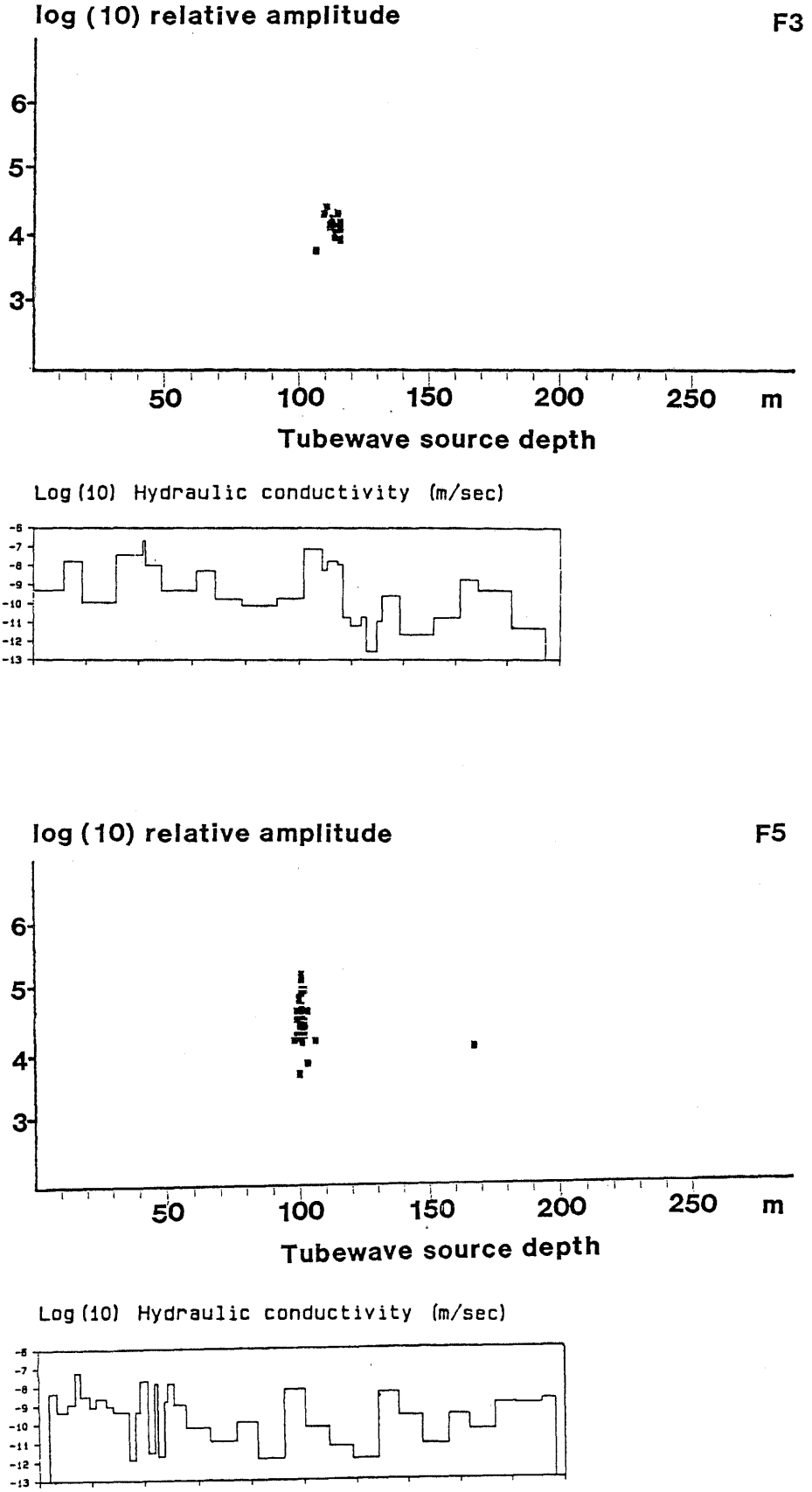


Figure 4-8 Tubewave relative amplitudes at different depths in F3 and F5 compared to hydraulic conductivity (1). Seismic source in F4, receiver in F3 (upper figure), receiver in F5 (lower fig

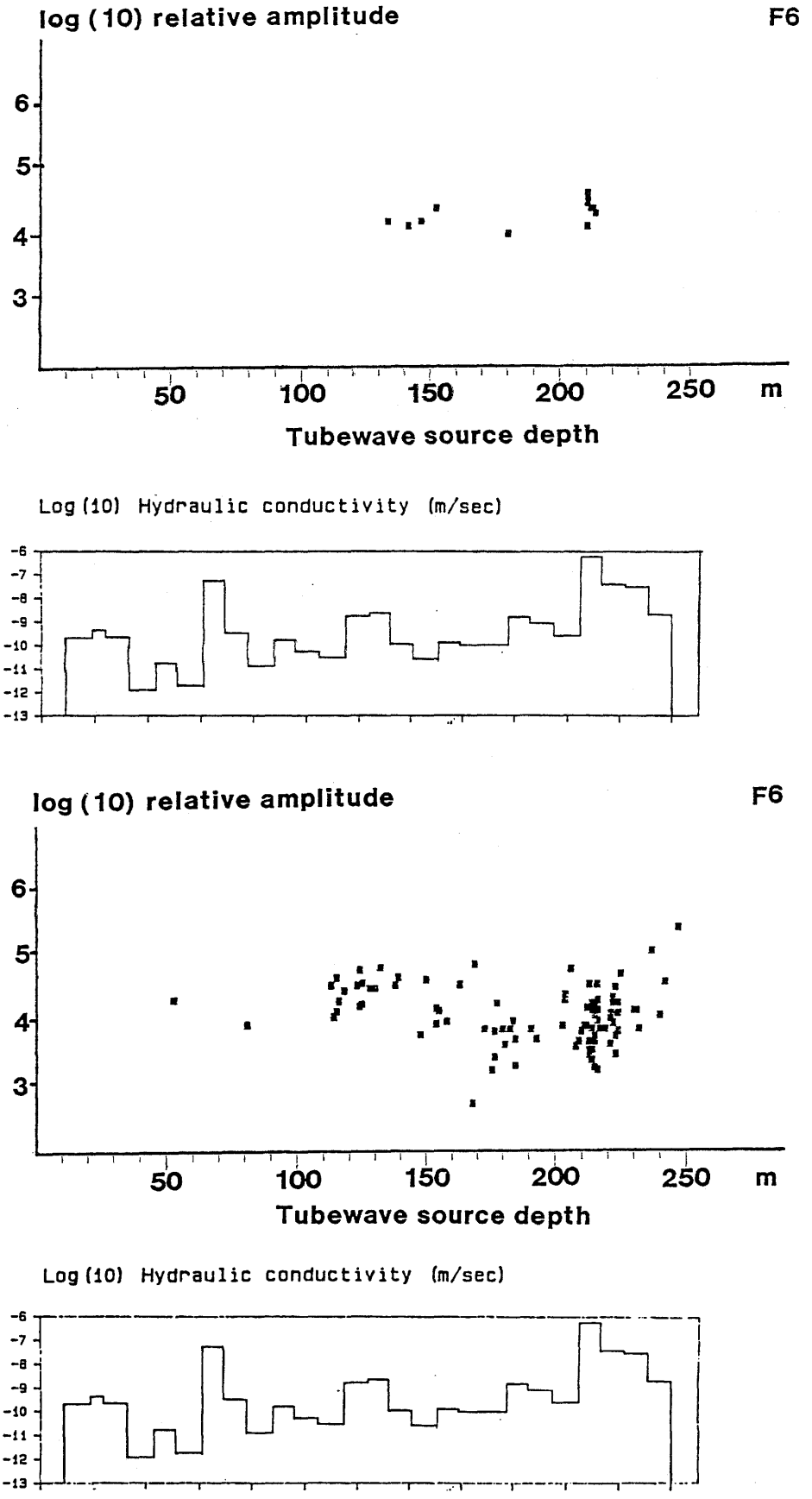


Figure 4-9 Tubewave relative amplitudes at different depths in F6 compared to hydraulic conductivity (1).
Seismic source in F4, receiver in F6 (upper figure).
" " in F5, receiver in F6 (lower figure).

# 4 GENERAL CONCLUSIONS

The techniques tested within this project show that it is possible to detect reflections from fractured zones in crystalline rock and to locate the reflectors.

Although a dense detector spread has to be used, the reflection method does not require more field work than tomography as only a few source positions are needed.

The effects of noise and interference with S-waves and tubewaves could be largely reduced and reflected P-waves were strongly emphasized.

The present exercise aimed at testing processing techniques on already existing data collected for tomographic processing. The test geometry and the frequency content of the recorded seismograms were therefore not quite appropriate for reflection analysis. With a more specialized routine for collecting data, the results would have been better.

The interpretations were focused on zone "C". This zone is consistently identified with all investigations methods, including reflection analysis. Zone "A" also gives rise to a reflection pattern. Other reflectors identified previously appear deeper in the boreholes and were not covered by the data set chosen for this study.

Even though the field configuration was not appropriate for tubewave analysis, tubewave phases could be resolved. It is shown that tubewave sources in most cases coincide with relatively higher hydraulic conductivity. In those cases where no correlation exists, the locations of the sources usually agrees with features found in radar and/or seismic measurements, (2,4,5).

The quantitative approach to correlate tubewave amplitudes with hydraulic conductivity (3.2.2), did not give an unambiguous result which could be due to interference from other tubewave phases and the varying physical conditions at different source and receiver positions. Thus the results obtained should be seen as a qualitative measure.

Analysis of tubewave phases can be used as a complement in crosshole measurements, to verify positions of fracture zones. As is the case with reflection analysis the results could be improved by having more recordings for each source position.

All the previously defined zones could be detected by tubewaves except zone "A", which appears in the uppermost part (around 40 m) in all the the boreholes. The absence of, or the difficulty in resolving, tubewaves from this zone is probably due to the source/receiver configuration and interfering effects from other phases.

# 5 REFERENCES


1. J.BLACK, "A preliminary appraisal of the single borehole hydraulic results of the crosshole project", Stripa Project Quarterly Report July-Septermber 1985, Appendix 1, SKB, Stockholm.

2. C.Cosma, "Crosshole Investigations Short and Medium Range Tomography", Stripa Project IR 1986.

3. C.F. Huang, J.A. Hunter "The correlation of "tube-wave" events with open fractures in fluid-filled boreholes; in Current Reasearch, Part A, Geological Survey of Canada, Paper 81-1A, p. 361-376, 1981.

4. M. Hammarström, S. Ivansson, P. Morén, J. Pihl, "Crosshole Investigations Results From Seismic Borehole Tomography", Stripa Project IR 1986.

5. O. Olsson, L. Falk, O. Forslund, L. Lundmark, E. Sandberg, "Crosshole Investigations - Results From Borehole Radar Investigations", Stripa Project IR 1986.

6. L. Stenberg, O. Olsson , "The tubewave method for identifying permeable fracture zones intersecting a borehole", SKB AR 84-14, SKB, Stockholm, Sweden.